AN IMPROVED SYNTHESIS OF SNO_2 SPHERICAL REDUCED GRAPHENE OXIDE AT LOW TEMPERATURE

Awang Nazrul A.M[1] (*ag_nazrul@hotmail.com*)
Sazmal E. Arshad[2] *(sazmal@ums.edu.my*)

[1]*Institut Pendidikan Guru Kampus Kent, Tuaran, 89200 Sabah, Malaysia*
[2]*Faculty of Science and Natural Resources, University Malaysia Sabah, 88400 Sabah, Malaysia*

ABSTRACT

An improved, cost effective and facile hydrothermal method was made for the synthesis of SnO_2 spherical reduced graphene oxide (rGO) composites (CPs), (SCGs) by using Teflon bottle based on one-step in situ reaction between tin (II) chloride and GO. As synthesis SCGs were characterized by Fourier transform infrared (FT-IR) spectroscopy, ultraviolet-visible (UV-vis) spectroscopy, and clearly confirmed by X-ray diffraction (XRD) with adjacent lattice fringe spacing of about 0.343 and 0.233 nm correspond to the (110) plane and (101) plane of the SnO_2 spherical, respectively. The spherical of SnO_2 were uniformly self-assembled on the surface of cuboid like rGO nanosheets has been confirmed by scanning electron microscopy (SEM).

Keywords: *Spherical, SnO_2, graphene, hydrothermal*

INTRODUCTION

Tin dioxide (SnO_2) is an n-type semiconductor and extensively used in solar cell (Snaith & Ducati, 2010), sensors (Mei, Chen, & Ma, 2014), rechargeable Li-ion batteries (LIBs) (Wang, Zhao, Liu, & Shen, 2014), optical electronic devices (Woo et. al., 2012), and catalyst (Santhi, Rani, & Karuppuchamy, 2016) applications. Meanwhile, some significant disadvantages largely limit the application of SnO_2 in various applications. Graphene is a 2D new allotrope of carbon has been emerged as a 'rising star' in material science as an excellent candidate for many applications (Geim & Novoselov, 2007). Depositing SnO_2 on graphene or rGO might alleviate the limitation occur due to conductive and stable support of graphene or rGO which has been reported earlier (Wang, Chen, Lacey, Xu, Xie, Li, Danner & Hu, 2018). From our best knowledge, until today there are several ways to synthesis SnO_2 spherical reduced graphene oxide (rGO) composites (CPs), (SCGs) and the most popular way is the hydrothermal method. Based on a reaction temperature, hydrothermal synthesis is classified into subcritical and supercritical synthetic reactions. Subcritical synthesis involves a temperature in the range of 100–240 °C, while in supercritical synthesis, the temperature could reach up to 1000 °C, and the pressure is up to 3000 bar.

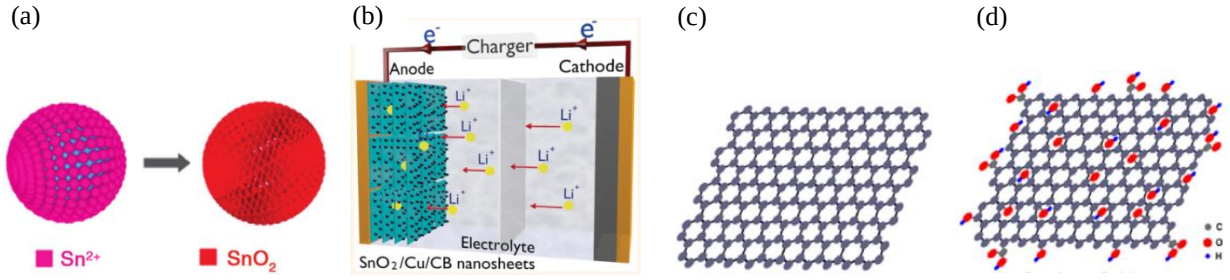

Figure 1. (a) Schematic illustration of the formation of the SnO_2 spheres (Chen, Wen and Lou, 2011). (b) Schematic configuration of a stacked SnO_2/Cu cell with multichannel design using CB as the spacer, which provides lithium ion and electron "superhighways" for charge storage and delivery. (Deng et.al., 2013). (c) Structural model of graphene. (d) Structural model of graphene oxide (GO) (Chen, Feng, and Li, 2012).

Under hydrothermal conditions (high temperature and pressure), water has several roles, such as (i) solvent; (ii) changing physical and chemical properties of reactants and products; (iii) accelerating reaction; (iv) participates in reaction, and (v) transferring pressure (Johnson and Arshad, 2014). Hydrothermal method is an alternative way to calcination for crystallization of metal oxide (SnO_2) at mild temperature and one of the best procedure to produce fine powder (Farrukh, et. al., 2010). In many works, Teflon-lined stainless steel autoclave is used during the reaction. However, the usage of an expensive autoclave is disadvantage of this method. Here in, we develop an improved,

economic and green hydrothermal method by using Teflon bottle (polypropylene bottle) at low temperature to synthesis SCGs from GO suspension, ethylene diamine (EDA) and Sn^{2+} for the first time.

EXPERIMENTAL

Preparation of GO (Graphene Oxide)

Graphene oxide was synthesized based on Improved Synthesis of Graphene Oxide with slight and an improved modification (Marcano, Kosynki, Berlin, Sinitskii, Sun, Slesarev, Alemany, Lu, and Tour, 2010). Briefly, a 9:1 mixture of concentrated H_2SO_4/H_3PO_4 (120:13.3 mL) is added to a mixture of graphite flakes (1.0 g) and $KMnO_4$ (6.0 g). The reaction was then heated to 50ºC and stirred for 24 h. The reaction was cooled to room temperature and poured onto ice (400 mL) with 30% H_2O_2 (8 mL) to obtain a graphite oxide (GrO) suspension. Later on, the mixture was centrifuged (5000 rpm for 20 mins). The remaining solid material was then washed in succession with 200 mL of 30% HCl for two times, and 200 mL of water for three times. For each wash, the mixture was centrifuged (5000 rpm for 20 mins) and obtains the GrO deposited (remaining material). Differ from the previous method, here in we introduce an improved extraction of GO from GrO. GrO was further diluted in 400 mL of deionized (DI) water, stirred for 12 hours and sonicated for 60 mins to obtain GO. The GO dispersion was the centrifuged at 5000 rpm for 30 min. The supernatant was collected and freeze-dried for 72 hours to obtain GO solid (flocculated GO).

Preparation of SCGs

Synthesis of SCGs based on Wang, Su, Park, Ahn, and Wang (2012) and Liang, Cai, Tian, Li, Geng and Guo (2013). In more detail, 2 g of $SnCl_2.2H_2O$ was firstly dissolved in 100 mL deionized water (DI) in a beaker and stirred for 10 mins. 40 mL of GO suspension (1 mg/mL) was added to 1 mL EDA then the mixture was added to the beaker contain $SnCl_2.2H_2O$ under continuous stirring for 30 mins. The mixture was transferred to a 250 ml Teflon bottle, which maintained in an oven at 120°C for 2 h. Afterwards, the black precipitates SCGs were collected, washed with DI and ethanol several times to remove the impurities, and isolated by gravity filtration. The product was then dried in an oven at 60°C for 5 hours.

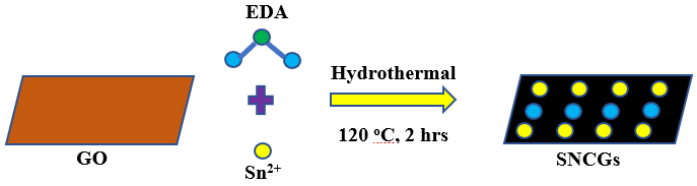

Figure 2. Schematic diagram the formation SCGs

Characterization

The powder X-ray diffraction (XRD) measurements of the samples were recorded on a Philips D8- Advance X-ray powder diffractometer by using a graphite monochromator with Cu KR radiation (λ) 1.5406 Å). The data were collected between scattering angles (2θ) of 5-80° at a scanning rate of 8°/min. Fourier-transform IR (FT-IR) spectra were carried out through a Perkin-Elmer spectrophotometer operating in the infrared domain 400-4000 cm^{-1}. The UV−vis absorption spectra of GO suspension and SCGs powder were recorded with an Agilent Cary60 UV−vis spectrophotometer. The microscopic morphology of SCGs powder was observed by Scanning Electron Microscope (SEM) (JSM-5610, Japan), with the acceleration voltage from 0.5 to 25KV.

RESULTS AND DISCUSSIONS

FTIR analysis of GO, SnO_2, and SCGs

The formation of GO, SnO_2, and SCGs was confirmed by the FTIR spectra (Figure 3). In the IR spectrum of GO (black line), the peak characteristic at 3337 cm^{-1} can be attributed to O–H stretching vibrations of adsorbed water molecules and structural OH groups. The characteristic peak at 1727 cm^{-1} corresponds to the stretching vibration of C=O, C-O vibrations (1155 cm^{-1}), O-C=O groups (875 cm^{-1}). The spectrum also depicts a peak at 1622 cm^{-1} which corresponds to C=C from unoxidized sp^2 CC bonds (Marcano et.al., 2010; Tang et. al., 2015). For the IR spectrum of SnO_2 (blue line), the bands at around 3000-3400 and 1635-1615 cm^{-1} which corresponds stretching vibrations of water molecules or hydroxide groups absorbed at the surface of the SnO_2. The band appeared at around 507-535 cm^{-1} consistent with Sn-OH stretching vibrations and formation of Sn-O (Farrukh, Heng and Adnan, 2010; Gnanam and

Rajendran, 2010; Abruzzi, Dedavid and Pires, 2015). Meanwhile, the introduction of Sn^{2+} ion eliminated most of oxygen-containing groups such as C=O peaks (1727 cm^{-1}), C-O stretching vibrations (1155 cm^{-1}), and O-C=O groups (875 cm^{-1}) for the IR spectrum of SCGs composite (red line). A strong peak at 523 cm^{-1} was assigned to Sn-OH or Sn-O. Further, a new wide absorption peak centered at 1167 cm^{-1} was observed in the IR of SCGs, which should be formation of Sn−O−C bonds in rGO (Liang, Cai, Tian, et.al., 2013). A new peak also appeared at approximately 1582 cm^{-1} which was believed to a skeletal vibration of graphene sheets (Tang et. al., 2015). The IR results indicate the reduction of GO to rGO (graphene) by Sn^{2+} and the Sn^{2+} oxidation to SnO_2 also confirming the existence of SCGs.

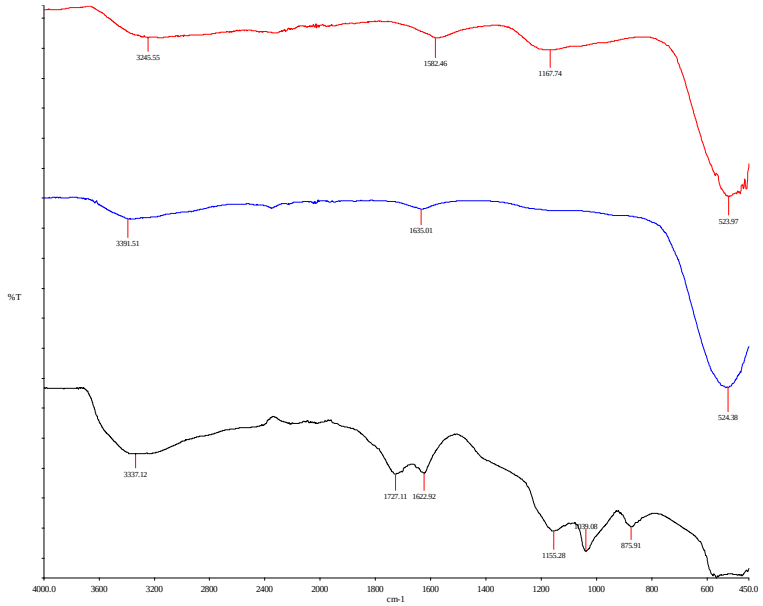

Figure 3. FTIR spectra of sample GO (black line), sample SnO_2 (blue line), and sample SCGs (red line).

XRD analysis of GO and SCGs

The structural properties of the SCGs were characterized and compared to the GO by XRD analysis (Figure 4). The GO diffraction peaks (Figure 4a) is observed at about 2Θ=8.0º is very typical for GO which is similar to that of Marcano, et.al. (2010), who had already described the structure of GO by XRD. The interlayer spacing of 1.13 nm resulting to facile exfoliation because of weakened the van der Waals forces between layers of GO (Li, et.al., 2010). On the other hand, an interlayer spacing showed a significant increase compare to its precursor in spacing is believed due to oxygen functional groups intercalate in the interlayer of graphite. There is a very weak diffraction peak at 43.7º, which is believed due to the incomplete oxidation (Cao and Zhang, 2014). For the sample of SCGs (Figure 4b), the diffraction peaks of layered GO around 8.0º was disappeared, which is indicates the successful reduction of GO by Sn^{2+} (Liang, et.al., 2013). The characteristics peaks of SnO_2 at 25.9º, 34.2º, 38.5º, 52.9º and 66.2º corresponding to the (110), (101), (200), (211), and (301), planes respectively of a tetragonal rutile-like phase of SnO_2 (JCPDS Card No. 41-1445) were observed in good agreement with those reported by Deosarkar, et.al. (2013) and Wang, et.al. (2014). It is indicates the high purity of the SnO_2 attached on the surfaces of graphene which is agreement with FTIR analysis (Liang, et. al., 2013). These diffraction peaks also considerably broadened, suggesting a small particle size of SnO_2 spherical crystallites with the lattice fringe spacing *d* (110) plane and (101) are 0.343 and 0.233 nm respectively which are similar reported by Li et.al. (2010). Moreover, the sharp diffraction peak at 25.9º of SCGs sample revealed crystalline nature of the nanomaterial formed with pure phase.

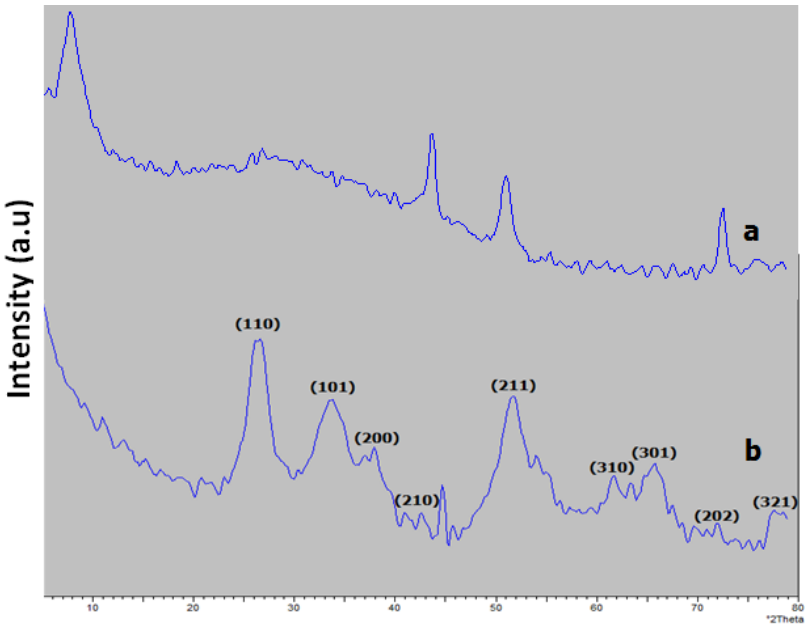

Figure 4. XRD pattern spectra of GO (a), sample SCGs (b).

Ultraviolet−Visible Spectroscopy Analysis of GO and SCGs

The UV–vis spectrum of GO (Figure 5a) shows the maximum peak absorption at 225 nm attributable to the π-π* transitions of the aromatic C–C bonds while the shoulder at around 300 nm is assigned to the n-π* transitions of the C=O bonds which are similar reported by Lim, Huang and Lim (2013) and Shariari and Atawale (2014). However, the peak at 225 nm right-shifted to 270 nm after the introduction of Sn^{2+} in the hydrothermal synthesis via Teflon bottle (Figure 5b) and the shoulder peak at 300 nm decreases in intensity, indicating the reduction of GO and the restoration of a p-conjugation network in the rGO. The missing 225 nm peak and the appearance of the 270 nm peak for SnO_2/rGO CPs agreement that GO had been reduced to rGO (graphene) (Chen, et. al., 2013). On the other hand, UV-Visible absorption spectrum was recorded in order to characterize the optical absorbance of the nanocrystalline SCGs. Figure 5b shows the optical absorbance spectra of SCGs. The band gap energy (Eg) for the SCGs can be obtained by recorded a strong cut off where the absorbance value is minimum (Dharma and Pisal, 2009). The minimum value absorbance of the sample SCGs was 386 nm (about 3.22 eV). It can be estimated by using the following equation:

Band gap energy (Eg) = hC/λ

h = Planks constant = 6.626 x 10^{-34} Js
C = Speed of light = 3.0 x 10^{8} m/s
λ = Cut off wavelength = 386 nm
Where 1 eV = 1.6 x 10-19 J

The obtained values are smaller than reported value for bulk SnO_2 (3.6eV) (Gnanam and Rajendran, 2010). It is consistent with the reported for the pristine graphene is zero band gap while for the chemically doped graphene result higher band gap. Introduction of Sn^{2+} influence the spin density and charge distribution of carbon atoms in graphene. Thus, it was believed the band gap between the conduction band and the valence band will be opened. The higher band gap in SCGs compare to pristine graphene makes it as a convenient candidate to be used in semiconductor devices (Wang, Maiyalagan and Wang, 2012).

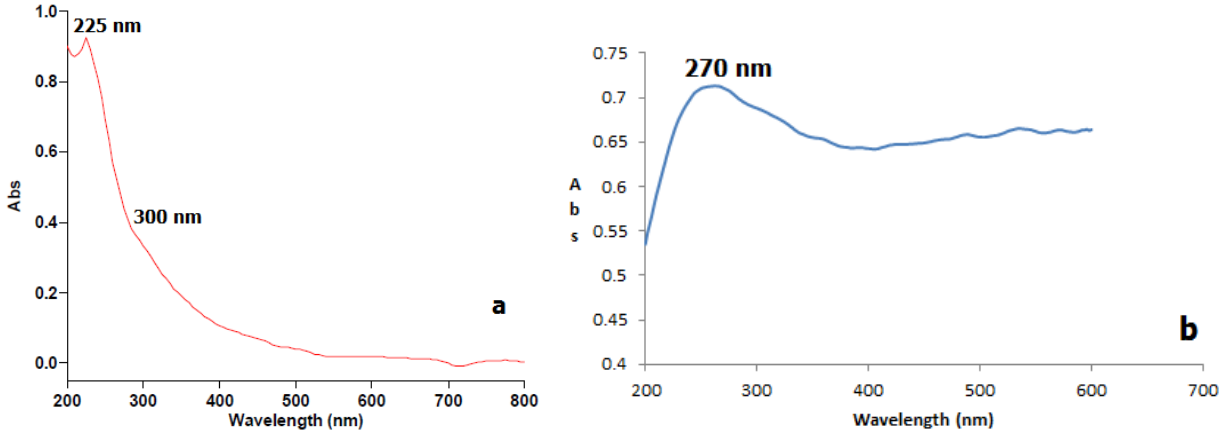

Figure 5. UV-vis spectrum of GO (a), sample SCGs (b).

Scanning Electron Microscope Analysis of GO and SCGs

The microscopic morphology of the as-synthesis SCG*s* samples was carried out by SEM analysis. The spherical like morphology of the SnO_2 spherical was shown clearly in Figure 6b revealed the crystallization of SnO_2 occurs at a low temperature at average size 100 nm. Upon addition of a $SnCl_2.2H_2O$ solution into a GO suspension, Sn^{2+} could be selectively bonded with the oxygen-containing groups through electrostatic force. Hydrolysis reaction between Sn^{2+} ions and OH^- leads to the formation of SnO_2. As reported earlier, EDA is a strong chelating agent that can readily coordinate with Sn^{2+}. Upon addition of EDA into the precursor mixture, complex $Sn_n(EDA)_m^{2+}$ is immediately formed, leading to decreased reactivity between Sn^{2+} and OH^- and formation of spherical SnO_2 crystallites. Meanwhile, the EDA also leads to N-doping of the graphene sheets as the GO is reduced into rGO (graphene) under the hydrothermal conditions (Liang, et.al., 2013). The tiny SnO_2 spherical also observed well-dispersed and anchored on the cuboid like rGO (graphene) sheets (Wang, et. al., 2012). It is noteworthy to mention that the Sn^+ has strong reducing influence on GO to be converted to rGO (graphene or Gr). Hence, formation of SnO_2 is accompanied with simultaneous reduction of GO that leads to the sought for SCGs as can be described by the following reactions (El-Deen, et. al., 2014):

$$Sn^{2+} + 2OH^- \longrightarrow Sn(OH)_2$$

$$Sn(OH)_2 + 2OH^- \longrightarrow SnO_2 + 2H_2O + 2e^-$$

$$GO + 2e^- \longrightarrow rGO$$

Overall reaction:

$$SnCl_2 + GO + H2O \longrightarrow rGO + SnO_2 + 2HCl$$

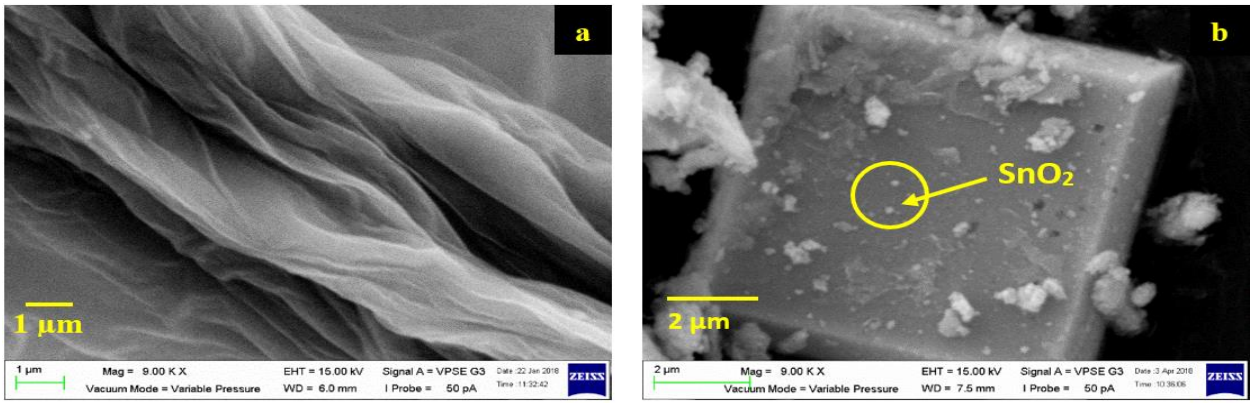

Figure 6. SEM image for layered structure, affords ultrathin, homogeneous, wrinkle, ripple and crumple graphene oxide films (a) SnO_2 spherical observed well-dispersed and anchored on the cuboid like rGO (graphene) SCGs (b)

After the hydrothermal reaction, the color of the solution changes from light brown to black, which confirms the successful reduction of GO to graphene (Liang, et.al., 2013). Further, graphene is believed acted as a support for SnO_2 spherical to prevent aggregation among the SnO_2 spherical which is agreement with FTIR analysis (Lim, Huang and Lim, 2013). Lim et.al. (2013) proposed that negatively charged GO nanosheets are added to positively charged Sn^{2+} (before hydrothermal). The Sn^{2+} ions are first coordinated onto the surface of the GO nanosheets due to the electrostatic interaction between the oppositely charged ions, which are the sites for nucleation. The GO acts as an oxidizing agent, oxidizing to Sn^{2+} to SnO_2 on the surface of GO, while GO will be simultaneously reduced to rGO (graphene) (after hydrothermal). These reactions result in the growth of SnO_2 spherical on the rGO nanosheets during the hydrothermal process.

CONCLUSIONS

An improved, facile, economic and green hydrothermal method by using Teflon bottle at low temperature has been developed to synthesis SCGs instead of conventional autoclave stainless steel method. The reduction of GO to rGO and the in situ formation of SnO_2 spherical were realized in one step, which provided a simple, low-cost, effective, and green strategy to prepare SCGs since no additional toxic chemicals were added. Water was involved in the formation of $Sn(OH)_2$, which resulted in the formation of SnO_2 spherical deposited on rGO. Moreover, introduction of EDA in this process, is believed resulting a formation of smallest SnO_2 spherical since EDA act as a ligand to control the morphology of the SnO_2 crystallites. The optical absorbance spectra result a wide band gap (3.2 eV) shows the as-synthesized SCGs provide better catalytic promote a better candidate applied in many research fields such as photocatalysis, gas sensor, optoelectronics and energy storage devices in future. Furthermore, this synthesis method could provide a facile, economic, and green strategy for the preparation of other metal-oxide/rGO CPs.

ACKNOWLEDGMENTS

This work was supported by Skim Geran Bantuan Penyelidikan Pascasiswazah (UMSGreat) Fasa 1/2016 GUG0033-SG-P-1/2016 University Malaysia Sabah.

REFERENCES

Abruzzi, R.C., Dedavid, B.A., Pires, M.J.R. 2015. Characterization of tin dioxide nanoparticles synthesized by oxidation. **61**(2015): 328-333.

Cao, N. and Zhang, Y. 2014. Study of Reduced Graphene Oxide Preparation by Hummers' Method and Related Characterization. *Journal of Nanomaterials.* **2015:** 1-5.

Chen, J. S., Archer, L. a., and Wen (David) Lou, X. 2011. SnO_2 Hollow Structures and TiO2 Nanosheets for Lithium-Ion Batteries. *Journal of Materials Chemistry*. **21**(27): 9912. http://doi.org/10.1039/c0jm04163g

Chen, D., Feng, H., and Li, J. 2012. Graphene Oxide: Preparation, Functionalization, and Electrochemical Applications. Chemical Review. **12**(2012): 6027 – 6053.

Chen, M., Zhang, C., Li, L., Liu, Y., Li, X., Xu, X., Xia, F., Wang, W., and Gao, J. 2013. Sn Powder as Reducing Agents and Sno2 Precursors for the Synthesis of Sno2-Reduced Graphene Oxide Hybrid nanoparticles. *ACS Applied Materials and Interfaces*. **5**(24): 13333–13339. http://doi.org/10.1021/am404195u

Deng, J., Yan, C., Yang, L., Baunack, S., Oswald, S., Wendrock, H., Mei, Y., and Schmidt, O.G. 2013. Sandwich-Stacked SnO_2/Cu Hybrid Nanosheets as Multichannel Anodes for Lithium Ion Batteries. *ACS Nano.* **7**(8): 6948 – 6954.

Deosarkar, M.P., Pawar, S.M., Sonawane, S.H., and Bhanvase. B.A. 2013. Process intensification of uniform loading of SnO2 nanoparticles on graphene oxide nanosheets using a novel ultrasound assisted in situ chemical precipitation method. Chemical Engineering and Processing: Process Intensification. **70**(2013): 48 – 54.

El-Deen, A.G., Barakat, N.A.M., Khalild, K.A., Motlak, M., and Kim, H.Y. 2014. Graphene/SnO_2 nanocomposite as an effective electrode material for saline water desalination using capacitive deionization. Ceramics International. **40**(2014): 14627-14634

Farrukh, M.A., Heng B-T., Adnanm R. 2010. Surfactant-controlled aqueous synthesis of SnO2 nanoparticles via the hydrothermal and conventional heating methods. Turkish Journal of Chemistry. 34 (2010). 537 – 550. doi:10.3906/kim-1001-466.

Gnanam, S. and Rajendran, V. 2010. Influence of ethylene glycol on the nanostructured pure and V-doped SnO2 nanoparticles via sol-gel process and application in photocatalysts. Journal of Optoelectronics and Advanced Materials. **12**(11). 2199-2207.

Geim, A.K., and Novoselov, K.S. 2007. The Rise of Graphene. *Nature Materials.* **6**(3): 183-191

Johnson, E.B.G., and Arshad, S.E. 2014. Hydrothermally synthesized zeolites based on kaolinite: A review. *Applied Clay Science.* **97 – 98**(2014): 215 – 221.

Li, Y., Lv, X., Lu, J., and Li, J. 2010. Preparation of SnO_2-Nanocrystal/Graphene-Nanosheets Composites and Their Lithium Storage Ability. *J. Phys. Chem. C*. **114:** 21770–21774. http://doi.org/10.1021/jp1050047

Liang, J., Cai, Z., Tian, Y., Li, L., Geng, J., and Guo, L. 2013. Deposition SnO2/Nitrogen-Doped Graphene Nanocomposites on the Separator: A New Type of Flexible Electrode for Energy Storage Devices. *ACS Applied Materials & Interfaces*. **5**(22): 12148-12155.

Lim, S.P., Huang, N.M., and Lim, H.N. 2013. Solvothermal synthesis of SnO_2/graphene nanocomposites for supercapacitor application. Ceramics International. **39**(6): 6647-6655.

Marcano, D. C., Kosynkin, D. V., Berlin, J. M., Sinitskii, A., Sun, Z., Slesarev, Alemany, Lu, and Tour, J. M. 2010. Improved Synthesis of Graphene Oxide. *ACS Nano*. **4**(8): 4806–4814. http://doi.org/10.1021/nn1006368

Santhi, K., Rani, C., and Karuppuchamy, S. 2016. Synthesis and Characterization of a Novel SnO/SnO2 Hybrid Photocatalyst. *Journal of Alloys and Compounds*. **662**: 102–107.

Snaith, H. J., and Ducati, C. 2010. SnO_2-Based Dye-Sensitized Hybrid Solar Cells Exhibiting Near Unity Absorbed Photon-to-Electron Conversion Efficiency. *Nano Letters*. **10**(4): 1259–1265. http://doi.org/10.1021/nl903809r

Tang, L., Nguyen, V.H., Lee, Y.R., Kim, J., and Shim, J-J. 2015. Photocatalytic activity of reduced graphene oxide/SnO2 nanocomposites prepared in ionic liquid. *Synthetic Metals.* **201**(2015):54-60.

Wang, Y., Chen, Y., Lacey, S.D., Xu, L., Xie, H., Li, T., Danner, V.A., and Hu, L. 2018. Reduced Graphene Oxide Film with Record High Conductivity and Mobility. *Materials Today.* Articles in Press. **(xx)**

Wang, H., Maiyalagan, T., and Wang, X. 2012. Review on Recent Progress in Nitrogen-Doped Graphene: Synthesis, Characterization, and Its Potential Applications. ACS Catalysis. **2**(5): 781 – 794.

Wang, B., Su, D., Park, J., Ahn, H., & Wang, G. 2012. Graphene-Supported SnO_2 Nanoparticles Prepared by a Solvothermal Approach for an Enhanced Electrochemical Performance in Lithium-ion Batteries. *Nanoscale Research Letters*. **7**(1): 215. http://doi.org/10.1186/1556-276X-7-215

Wang, X., Zhao, C., Liu, R., and Shen, Q. 2014. Hydrothermal Synthesis and Structural Properties of Hierarchical Flower-like SnO_2 Nanostructures for Lithium Ion Batteries. *Journal of Nanoparticle Research.* **16**(8):1-8. http://doi.org/10.1007/s11051-014-2570-4

Woo, H.-S., Hwang, I.-S., Na, C. W., Kim, S.-J., Choi, J.-K., Lee, J.-S., Choi, J., Kim, J.T., and Lee, J.-H. 2012. Simple Fabrication of Transparent Flexible Devices Using SnO2 Nanowires and Their Optoelectronic Properties. *Materials Letters*. **68:** 60–63. http://doi.org/10.1016/j.matlet.2011.10.016